AIP | Applied Physics Letters

Atomic arrangements of (Ga1−xMnx)N nanorods grown on Al2O3 substrates

K. H. Lee, J. Y. Lee, J. H. Jung, T. W. Kim, H. C. Jeon et al.

Citation: Appl. Phys. Lett. **92**, 141919 (2008); doi: 10.1063/1.2902321
View online: http://dx.doi.org/10.1063/1.2902321
View Table of Contents: http://apl.aip.org/resource/1/APPLAB/v92/i14
Published by the American Institute of Physics.

Atomic arrangements of $(Ga_{1-x}Mn_x)N$ nanorods grown on Al_2O_3 substrates

K. H. Lee,[1] J. Y. Lee,[1] J. H. Jung,[2] T. W. Kim,[2,a)] H. C. Jeon,[3] and T. W. Kang[3]
[1]*Department of Materials Science and Engineering, Korea Advanced Institute of Science and Technology, Daejeon 305-701, Republic of Korea*
[2]*Advanced Semiconductor Research Center, Division of Electronics and Computer Engineering, Hanyang University, 17 Haengdang-dong, Seongdong-gu, Seoul 133-791, Republic of Korea*
[3]*Quantum-functional Semiconductor Research Center and Department of Physics, Dongguk University, Seoul 100-715, Republic of Korea*

(Received 26 May 2007; accepted 6 March 2008; published online 11 April 2008)

X-ray diffraction (XRD) and selected area electron diffraction pattern (SADP) results showed that the $(Ga_{1-x}Mn_x)N$ nanorods had preferential *c*-axial growth direction. Transmission electron microscopy (TEM) and high-resolution TEM (HRTEM) images showed that one-dimensional $(Ga_{1-x}Mn_x)N$ nanorods without defects had *c*-axis-oriented crystalline wurzite structures. Atomic arrangements for the $(Ga_{1-x}Mn_x)N$ nanorods grown on the Al_2O_3 (0001) substrates are described on the basis of the XRD, the TEM, the SADP, and the HRTEM results. © *2008 American Institute of Physics*. [DOI: 10.1063/1.2902321]

Diluted magnetic semiconductor (DMS) quantum structures utilizing both ferromagnetic and semiconductor nanostructures have been attractive because of interest in investigations of fundamental physics[1–3] and their potential applications in spintronic devices.[4–6] Among the various kinds of DMS materials, $(Ga_{1-x}Mn_x)As$ DMS thin films grown on GaAs substrates have been the most extensively studied materials.[7–10] However, until now, the highest ferromagnetic transition temperature (T_c) obtained from III-V DMS thin films has been 172 K;[11] thus, various studies concerned with increasing the T_c of DMS materials have made extensive efforts with the goal of obtaining spintronic devices operating at room temperature. Among the various kinds of DMS materials with a room temperature T_c, $(Ga_{1-x}Mn_x)N$ DMSs have become particularly interesting because they are theoretically expected to have high values for T_c.[12] Some works concerning the growth and characterization of $(Ga_{1-x}Mn_x)N$ DMSs with a very high T_c have been performed.[13–18] Recently, some works on the formation of $(Ga_{1-x}Mn_x)N$ nanowires have been reported,[19,20] but systematic studies concerning the microstructural properties and atomic arrangements of the $(Ga_{1-x}Mn_x)N$ nanorods grown on Al_2O_3 (0001) substrates have not yet been performed. Because the microstructural properties and atomic arrangements of the $(Ga_{1-x}Mn_x)N$ nanorods significantly affect the electrical, magnetic, and optical properties of the nanorods that are necessary to fabricate high-efficiency devices, studies of the microstructural properties and atomic arrangements of $(Ga_{1-x}Mn_x)N$ nanorods are very important for spintronic devices based on such properties.

This letter reports data regarding the microstructural properties and atomic arrangements of $(Ga_{1-x}Mn_x)N$ nanorods grown on Al_2O_3 (0001) substrates by using molecular beam epitaxy (MBE). x-ray diffraction (XRD), transmission electron microscopy (TEM), selected area diffraction pattern (SADP), and high-resolution TEM (HRTEM) measurements were carried out to characterize the microstructural properties of the $(Ga_{1-x}Mn_x)N$ nanorods grown on Al_2O_3 (0001) substrates. Energy dispersive spectroscopy (EDS) measurements were performed to determine the composition of the $(Ga_{1-x}Mn_x)N$ nanorods. Atomic arrangements for the $(Ga_{1-x}Mn_x)N$ nanorods grown on Al_2O_3 (0001) substrates are described on the basis of the XRD, the TEM, the SADP, and the HRTEM results.

The $(Ga_{1-x}Mn_x)N$ nanorods used in this study were grown on Al_2O_3 (0001) substrates by using a rf-associated MBE system. The deposition of the $(Ga_{1-x}Mn_x)N$ nanorods was done at a substrate temperature of 600 °C. The XRD measurements were performed by using a D/MAX-RC (12 kW) diffractometer with Cu $K\alpha$ radiation. The TEM measurements were performed by using JEOL JEM 2000EX and JEOL JEM 3010 microscopes operating at 200 and 300 kV, respectively. The samples for the cross-sectional TEM measurements were prepared by cutting and polishing with diamond paper to a thickness of approximately 20 μm and then argon-ion milling at liquid-nitrogen temperature to electron transparency.

Figure 1 shows the XRD for the $(Ga_{1-x}Mn_x)N$ nanorods grown on Al_2O_3 (0001) substrates. The dominant (0002) $K\alpha$ diffraction peak corresponding to the $(Ga_{1-x}Mn_x)N$ nanorods together with the (0006) $K\alpha$ diffraction peak corresponding to the Al_2O_3 substrate are clearly observed in Fig. 1. The

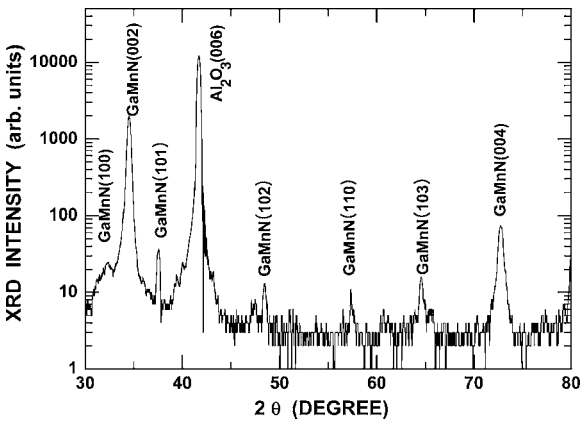

FIG. 1. X-ray diffraction curve of the $(Ga_{1-x}Mn_x)N$ nanorods grown on Al_2O_3 (0001) substrates, which is plotted in a logarithm scale.

a)Author to whom correspondence should be addressed. Electronic mail: twk@hanyang.ac.kr.

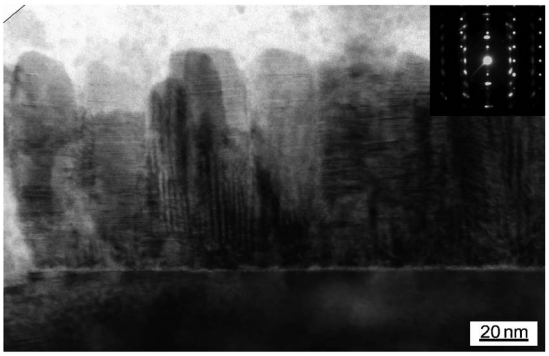

FIG. 2. Bright-field transmission electron microscopy image of the $(Ga_{1-x}Mn_x)N$ nanorods grown on the Al_2O_3 (0001) substrates. The inset indicates a selected area electron diffraction pattern, taken along the $[2\bar{1}\bar{1}0]$ zone axis of the $(Ga_{1-x}Mn_x)N$ nanorods.

XRD pattern for the $(Ga_{1-x}Mn_x)N$ nanorods grown on Al_2O_3 (0001) substrates indicates that the $(Ga_{1-x}Mn_x)N$ nanorods have a wurzite structure with a strong *c*-axis orientation, the orientation which gives the lowest surface free energy.[21] Because the low-index surface of the (0001) plane in the $(Ga_{1-x}Mn_x)N$ nanorods has the largest energy,[22] the $(Ga_{1-x}Mn_x)N$ nanorods have a *c*-axis preferential orientation in the [0001] direction. Several peaks at 32°, 37°, 48°, 57°, 64°, and 73° with a small intensity are observed in the XRD pattern shown in Fig. 1. The subordinate peaks at around 32°, 37°, 48°, 57°, 64°, and 73° might be attributed to the $(10\bar{1}0)$, $(10\bar{1}1)$, $(10\bar{1}2)$, $(11\bar{2}0)$, $(10\bar{1}3)$, and (0004) $(Ga_{1-x}Mn_x)N$ planes, respectively. Most nucleation sites at an initial stage were formed to (0001) preferential orientations; exceedingly small nucleation sites with a different orientation, such as $(10\bar{1}1)$ planes, are formed at the initial formation stage of the $(Ga_{1-x}Mn_x)N$ nanorods, which is clarified by HRTEM images of the $(Ga_{1-x}Mn_x)N$ nanorod/Al_2O_3 (0001) substrate interface region with a different orientation. Because the low-index surface of the (0001) plane in the $(Ga_{1-x}Mn_x)N$ nanorods has the largest energy, these nuclei with a different orientation gradually disappear, resulting in the formation of the $(Ga_{1-x}Mn_x)N$ nanorods that have a *c*-axis preferential orientation in the [0001] direction.

Figure 2 shows a bright-field TEM image of $(Ga_{1-x}Mn_x)N$ nanorods grown on an Al_2O_3 (0001) substrate. The widths of the $(Ga_{1-x}Mn_x)N$ nanorod are approximately 10–20 nm, and their heights are about 50–60 nm, as shown in Fig. 2. After the $(Ga_{1-x}Mn_x)N$ thin films with thicknesses between 10 and 20 nm are two-dimensionally grown on Al_2O_3 (0001) substrates during the initial growth stage, $(Ga_{1-x}Mn_x)N$ nanorods are one-dimensionally grown on $(Ga_{1-x}Mn_x)N$ thin films. Because the growth temperature (600 °C) of the $(Ga_{1-x}Mn_x)N$ nanorods grown by Al_2O_3 (0001) substrates by using MBE is much lower than the temperature (about 800 °C) of the $(Ga_{1-x}Mn_x)N$ thin films grown on Al_2O_3 (0001) substrates by using MBE, the $(Ga_{1-x}Mn_x)N$ nanorods with an one-dimensional structure can be formed. The formation of $(Ga_{1-x}Mn_x)N$ nanorods is attributed to an significant increase in the compressive strain of the $(Ga_{1-x}Mn_x)N$ layer at an initial growth stage resulting from the low thermal energy due to the low temperature growth. The inset of Fig. 2 shows a SADP from the $(Ga_{1-x}Mn_x)N$ nanorods grown on an Al_2O_3 (0001) substrate. The orientation relationships between the Al_2O_3 (0001) substrates and the $(Ga_{1-x}Mn_x)N$ nanorods are $(0001)_{Al_2O_3} \| (0001)_{(Ga_{1-x}Mn_x)N}$ and $[1\bar{1}00]_{Al_2O_3} \| [2\bar{1}\bar{1}0]_{(Ga_{1-x}Mn_x)N}$. The large lattice mismatch between the $(Ga_{1-x}Mn_x)N$ nanorods and the Al_2O_3 (0001) substrates (about 16%) induces a large compressive stress at the heterointerface region. The streaks in the SADP corresponding to the $(Ga_{1-x}Mn_x)N$ nanorods indicate that $(Ga_{1-x}Mn_x)N$ nanorods grown on Al_2O_3 substrates have a slightly tilted *c*-axis orientation. The measured lattice constants of the *a* and the *c* axes for the $(Ga_{1-x}Mn_x)N$ nanorods are slightly decreased but are little different from those of the bulk GaN materials. Because the Mn ions for the Mn-implanted GaN materials are located at or near the Ga site,[23] the decrease in the lattice constant of the $(Ga_{1-x}Mn_x)N$ nanorod originates from the substitution of Mn atoms into Ga sites.

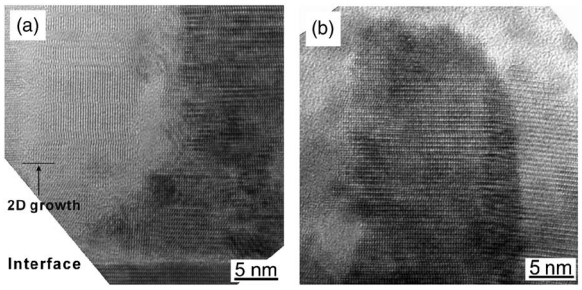

FIG. 3. High-resolution transmission electron microscopy images of (a) the $(Ga_{1-x}Mn_x)N$ nanorod/Al_2O_3 (0001) substrate heterointerface region and (b) the tip region of the nanorods.

In the EDS measurements, the atomic distribution of the Mn atoms was uniform throughout the $(Ga_{1-x}Mn_x)N$ nanorods. The EDS spectrum of the nanorod-tip regions demonstrates that the stoichiometry of the nanorods is $(Ga_{1-x}Mn_x)N$ and that the ratio between the Ga and the Mn compositions is 95:5.

Figure 3 shows a HRTEM image of (a) the $(Ga_{1-x}Mn_x)N$ nanorods/Al_2O_3 (0001) substrate heterointerfaces and (b) the tip region of the $(Ga_{1-x}Mn_x)N$ nanorods. The HRTEM image shows that the $(Ga_{1-x}Mn_x)N$ was two-dimensionally grown near the interfacial region during the initial growth stage, as shown in Fig. 3(a). One-dimensional $(Ga_{1-x}Mn_x)N$ nanorods were roughly formed on two-dimensional thin films with a thickness of 10 nm. Figures 3(a) and 3(b) indicate that the growth direction of the $(Ga_{1-x}Mn_x)N$ nanorods was parallel to the [0001] direction. This result is in reasonable agreement with the XRD and the SADP results. $(Ga_{1-x}Mn_x)N$ nanorods do not contain defects except for stacking faults. Although the space between the $(Ga_{1-x}Mn_x)N$ nanorods is shown to be filled with some materials, the space is certainly vacuum, which is clarified from the top-view SEM image of the samples. Electron beams in the TEM are transmitted to the parallel to the Al_2O_3 (0001) substrate. Several nanorods can be existed in the pass of the electron beam because of the $(Ga_{1-x}Mn_x)N$ nanorods with a diameter of about 20 nm and of the TEM sample with a thickness of approximately 100 nm. Out of focused $(Ga_{1-x}Mn_x)N$ nanorods or epoxy used to prepare the TEM sample might be shown to be different materials in HRTEM image.

Figure 4(a) shows the magnified HRTEM image of the $(Ga_{1-x}Mn_x)N/Al_2O_3$ heterointerface region. The HRTEM image shows that the orientation relationships

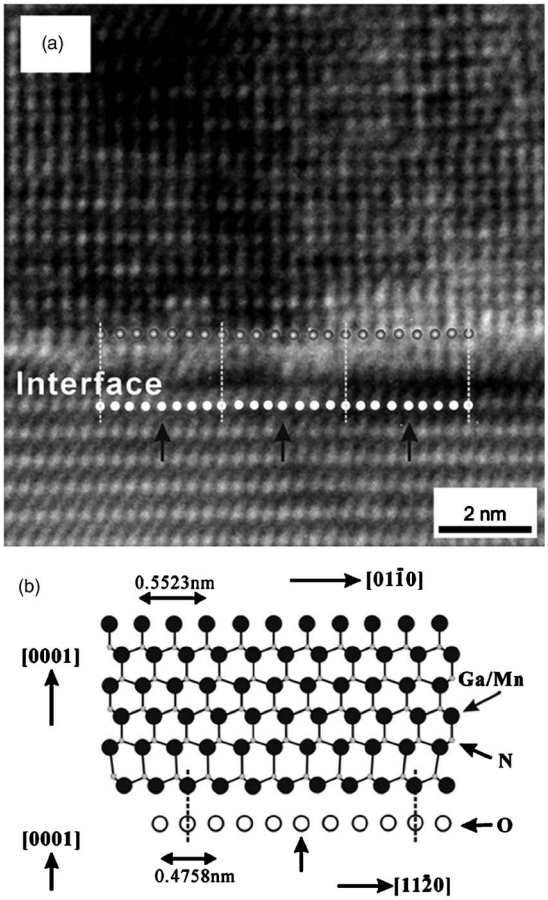

FIG. 4. (a) High-resolution transmission electron microscopy image of the interface region. The arrows indicate the extra half planes at a heterointerface. (b) Atomic arrangements for the $(Ga_{1-x}Mn_x)N$ nanorods grown on the Al_2O_3 (0001) substrate.

between the Al_2O_3 substrates and the $(Ga_{1-x}Mn_x)N$ nanorods are $(0001)_{Al_2O_3}\|(0001)_{(Ga_{1-x}Mn_x)N}$ and $[1\bar{1}00]_{Al_2O_3}\|[2\bar{1}\bar{1}0]_{(Ga_{1-x}Mn_x)N}$. The lattice mismatch between the Al_2O_3 (0001) substrate and the $(Ga_{1-x}Mn_x)N$ layer is approximately 16%. Because the lattice constant of the $(Ga_{1-x}Mn_x)N$ nanorods is larger than that of the Al_2O_3 (0001) substrate, a large compressive stress is induced to the $(Ga_{1-x}Mn_x)N$ thin film region. Even though the $(Ga_{1-x}Mn_x)N$ thin film near the heterointerface is strained to coherently grow to the substrate, the misfit dislocations are created due to large lattice mismatch. The arrows in Fig. 4(a) indicate the extra half planes at a heterointerface. Misfit dislocations were regularly created, as shown in Fig. 4(a) and atomic arrangements of the $(Ga_{1-x}Mn_x)N$ nanorods grown on the Al_2O_3 (0001) substrate are shown in Fig. 4(b). The regular misfit dislocations, indicated by the arrows in Fig. 4(b), are formed due to the lattice mismatch between the Al_2O_3 (0001) substrate and the $(Ga_{1-x}Mn_x)N$ layer.

In summary, $(Ga_{1-x}Mn_x)N$ nanorods were grown on Al_2O_3 (0001) substrates by using MBE. The XRD and the bright-field TEM results showed that the $(Ga_{1-x}Mn_x)N$ nanorods grown on Al_2O_3 (0001) substrates had uniform morphologies with a *c*-axis preferential orientation in the [0001] crystal direction. The XRD and SADP results showed that the lattice constant of the $(Ga_{1-x}Mn_x)N$ nanorods was slightly decreased compared to that of the GaN bulks, indicative of the substitution of Mn atoms into Ga sites. The HRTEM images showed that the $(Ga_{1-x}Mn_x)N$ nanorods did not contain defects except for stacking faults. Atomic arrangements for the $(Ga_{1-x}Mn_x)N$ nanorods grown on a Al_2O_3 (0001) substrate are described on the basis of the XRD, the TEM, and the HRTEM results.

This work was supported by the Korea Science and Engineering Foundation through the Quantum-functional Semiconductor Research Center at Dongguk University and by a Grant (No. 07K1501-01210) from the Center for Nanostructured Materials Technology under 21st Century Frontier R&D Programs of the Ministry of Science and Technology, Korea. This work was also supported by the Korea Science and Engineering Foundation (KOSEF) grant funded by the Korea government (MOST) (No. R0A-2007-000-20044-0).

[1] Y. Ohno, D. K. Young, B. Beschoten, F. Matsukura, H. Ohno, and D. D. Awschalom, Nature (London) **402**, 790 (1999).
[2] H. Ohno, Science **281**, 951 (1998).
[3] H. Munekata, A. Zaslavsky, P. Fumagalli, and R. J. Ganbino, Appl. Phys. Lett. **63**, 2929 (1993).
[4] H. Ohno, A. Shen, F. Matsukura, A. Oiwa, A. Endo, S. Katsumoto, and Y. Iye, Appl. Phys. Lett. **69**, 363 (1996).
[5] S. D. Sarma, Nat. Mater. **2**, 292 (2003).
[6] I. Malajovich, J. J. Berry, N. Samarth, and D. D. Awschalom, Nature (London) **411**, 770 (2001).
[7] S. Koshihara, A. Oiwa, M. Hirasawa, S. Katsumoto, Y. Iye, C. Urano, H. Takagi, and H. Munekata, Phys. Rev. Lett. **78**, 4617 (1998).
[8] T. Hayashi, M. Tanaka, K. Seto, T. Nishinaga, and K. Ando, Appl. Phys. Lett. **71**, 1825 (1997).
[9] S. J. Potashnik, K. C. Ku, S. H. Chun, J. J. Berry, N. Samarth, and P. Schiffer, Appl. Phys. Lett. **79**, 1495 (2001).
[10] D. Chiba, K. Takamura, F. Matsukura, and H. Ohno, Appl. Phys. Lett. **82**, 3020 (2003).
[11] A. M. Nazmul, S. Sugahara, and M. Tanaka, Phys. Rev. B **67**, 241308 (2003).
[12] T. Dietl, H. Ohno, F. Matsukura, J. Cibert, and D. Ferrand, Science **287**, 1019 (2000).
[13] S. Sonoda, S. Shimizu, T. Sasaki, Y. Yamamoto, and H. Hori, J. Cryst. Growth **237-239**, 1358 (2002).
[14] G. T. Thaler, M. E. Overberg, B. Gila, R. Frazier, C. R. Abernathy, S. J. Pearton, J. S. Lee, S. Y. Lee, Y. D. Park, Z. G. Khim, J. Kim, and F. Ren, Appl. Phys. Lett. **80**, 3964 (2002).
[15] T. Graf, M. Gjukic, M. S. Brandt, M. Stutzmann, and O. Ambacher, Appl. Phys. Lett. **81**, 5159 (2002).
[16] A. Y. Polyakov, A. V. Govorkov, N. B. Smimov, N. Y. Pashkova, G. T. Thaler, M. E. Overberg, R. Frazier, C. R. Abernathy, S. J. Pearton, J. Kim, and F. Ren, J. Appl. Phys. **92**, 4989 (2002).
[17] K. Sardar, A. R. Raju, B. Bansal, V. Venkataraman, and C. N. R. Rao, Solid State Commun. **125**, 55 (2003).
[18] M. Hashimoto, Y. K. Zhou, H. Tampo, M. Kanamura, and H. Asahi, J. Cryst. Growth **252**, 499 (2003).
[19] H. J. Choi, H. K. Seong, J. Y. Chang, K. I. Lee, Y. J. Park, J. J. Kim, S. K. Lee, R. He, T. Kuykendall, and P. Yang, Adv. Mater. (Weinheim, Ger.) **17**, 1351 (2005).
[20] Y. P. Song, P. W. Wang, X. H. Zhang, and D. P. Yu, Physica B **368**, 16 (2005).
[21] N. Fujimura, T. Nishhara, S. Goto, J. Xua, and T. Ito, J. Cryst. Growth **130**, 269 (1993).
[22] L. E. Greene, M. Law, D. H. Tan, M. Montano, J. Goldberger, G. Somorjai, and P. Yang, Nano Lett. **5**, 1231 (2005).
[23] C. Liu, E. Alves, A. R. Ramos, M. F. da Silva, J. C. Soares, T. Matsutani, and M. Kiuchi, Nucl. Instrum. Methods Phys. Res. B **191**, 544 (2002).